Characterization of GFDM Signal with Timing Offset, CFO, Non-Linearity, and PN

Fereshteh Yazdani (fereshte.yazdani@aut.ac.ir)
Amirkabir University https://orcid.org/0000-0002-3934-6549
Abbas Mohammadi
Amirkabir University
Abdolali Abdipour
Amirkabir University
Mohammad Kazemi
Amirkabir University

Research Article

Keywords: Timing offset, Carrier frequency offset, Nonlinear power amplifier distortion, phase noise, OFDM, GFDM

Posted Date: November 1st, 2021

DOI: https://doi.org/10.21203/rs.3.rs-747120/v1

Noname manuscript No.
(will be inserted by the editor)

Characterization of GFDM Signal with Timing Offset, CFO, Non-Linearity, and PN

Fereshteh Yazdani · Abbas Mohammadi · Abdolali Abdipour · Mohammad Kazemi

the date of receipt and acceptance should be inserted later

Abstract In this paper, we study the joint effects of timing offset (TO), carrier frequency offset (CFO), nonlinear power amplifier distortion, and phase noise (PN) on generalized frequency division multiplexing (GFDM) system. Closed form expressions for signal-to-interference ratio (SIR) at GFDM receiver with synchronization errors and PN using a nonlinear power amplifier is derived. Then, we have been conducted simulation studies to compare the performance of GFDM systems with orthogonal frequency division multiplexing (OFDM) systems using matched filter (MF) and zero forcing (ZF), in presence of these impairments. The results show that GFDM systems are more robust against TO and PN while they are more sensitive to CFO and nonlinear distortion compared to OFDM systems.

Keywords Timing offset · Carrier frequency offset · Nonlinear power amplifier distortion · phase noise · OFDM · GFDM

1 Introduction

The fifth generation of mobile communications (5G) includes a variety of applications such as machine-to-machine (M2M) communication, internet of things (IoT), and cognitive radio. The higher data rate, lower out-of-band (OOB) emission, low peak-to-average power ratio (PAPR), and higher spectral efficiency are vital to the implementing of these applications.[1,2,3] Orthogonal frequency division multiplexing (OFDM) is the most common multicarrier technique utilized in modern communication systems. Despite OFDM's numerous advantages, it has critical problems such as sensitivity to synchronization errors and high OOB emissions. Therefore, the use of OFDM for 5G needs to be reconsidered.[4,5] Generalized frequency division multiplexing (GFDM)[6] is a promising candidate waveform for 5G. In this paper, we consider the GFDM waveform, which is based on the modulation of independent blocks and offers a highly flexible time-frequency structure. Since GFDM is flexible in pulse shaping, its out-of-band emission and interference can be less than OFDM.[8] Moreover, GFDM has better spectral efficiency than OFDM. GFDM utilizes only one cyclic prefix for each block[6].

Phase noise (PN), timing offset (TO), carrier frequency offset (CFO), and nonlinear power amplifier cause inter subcarrier interference (ICI), inter subsymbol interference (ISI), and nonlinear distortion, which are produced by symbol starting point estimation, Doppler shift, non-ideal and mismatched oscillators, and nonlinear power amplifier, respectively, which reduce the signal to interference ratio (SIR) of the system.[9] In[10], the SIR for OFDM systems with TO is presented while the authors in[11] derive closed-form expressions for SIR with PN, CFO, and doubly selective fading. Also, authors in[12] provide SIR for uplink orthogonal frequency division multiple access (OFDMA) with large timing/carrier frequency offsets. The SIR of the output signal of non-linear

Fereshteh Yazdani
Department of Electrical Engineering, Amirkabir University, Tehran, Iran
Tel.: +98-21-64540
E-mail: fereshte.yazdani@aut.ac.ir

power amplifier for OFDMA is derived in[13], considering a non-uniform power distribution in subcarriers. In recent years, the impacts of some RF impairments on the GFDM waveforms have been studied. In[14], the SIR performance of GFDM and OFDM systems are compared with frequency and timing errors. Also, the SIR for OFDM and GFDM signals with PN, CFO, and TO is analyzed in[15]. In[16] SINR of GFDM Systems under I/Q imbalance is provided while the analysis of SIR with PN, CFO, and I/Q imbalance is investigated in[17]. The author in[18] derives the optimal filter for a GFDM system with CFO. For a third-order nonlinear power amplifier, the signal-to interference-plus noise ratio (SINR) for GFDM signal is studied in[19]. Despite all these efforts, however, the joint impact of TO, CFO, nonlinear power amplifier distortion, and PN on the performance of GFDM systems has not been investigated. Therefore, in this paper, joint impact of TO, CFO, nonlinear power amplifier distortion, and PN on the performance of GFDM waveform is analyzed. Assuming a polynomial model for the nonlinear behavior of power amplifier we derive closed-form expressions for SIR of GFDM signal under these impairments.

The rest of this paper is organized as follows. The GFDM system model is given in Section II. The SIR of GFDM signal with nonlinear power amplifier with synchronization errors and PN is obtained in Section III. Simulation results are presented in Section IV. Finally, this paper is concluded in Section V.

Notations: Vectors and matrices are represented by lower and upper case fonts (e.g. $\vec{x}$ and X), respectively. $E[\cdot]$, $(\cdot)^*$, $(\cdot)^H$, $(\cdot)^T$, and $(\cdot)^{-1}$ are the expectation, conjugate, Hermitian, transpose, and inverse operator, respectively. $diag(X)$ represents a column vector of the main diagonal elements of the matrix X. $\otimes$ and $\circ$ are convolution and Hadamard operators. The $N \times N$ identity matrix, $N \times N$ zero matrix, $m \times n$ zero matrix, and all one column vector of size N are denoted by I_N, 0_N, $0_{m\times n}$, and 1_N, respectively.

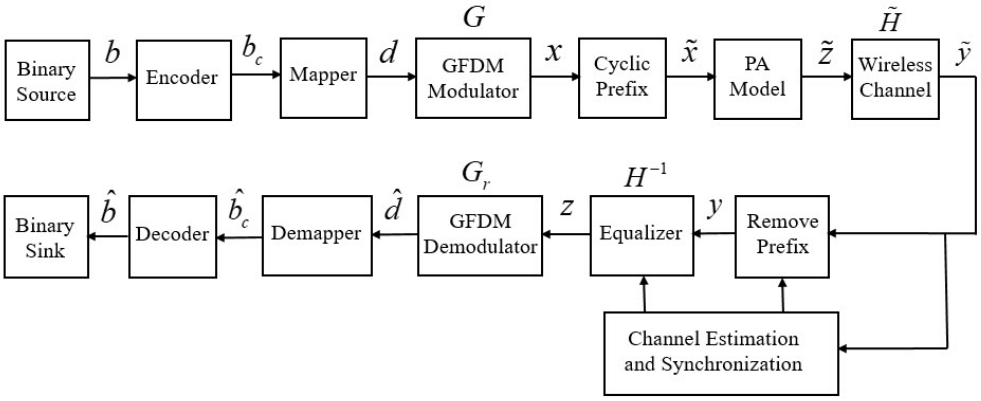

Fig. 1 A GFDM communication system.

2 SIGNAL AND SYSTEM MODEL

Fig. 1 depicts different parts of a GFDM system. A binary source provides the binary data vector $\vec{b}$ to produce the encoded data vector $\vec{b}_c$ by the encoder. A mapper, (e.g., PSK) maps the encoded bits to symbols. After mapping, we obtain vector $\vec{d} = \left(\vec{d}_0^T, \ldots, \vec{d}_{M-1}^T\right)^T$, which contains $N = MK$ independent and identically distributed (i.i.d) complex data symbols, where M denotes the number of subsymbols, K denotes the number of subcarriers, $\vec{d}_0 = \left(\vec{d}_{0,0}^T, \ldots, \vec{d}_{K-1,0}^T\right)^T$, and $\vec{d}_m = \left(\vec{d}_{0,m}^T, \ldots, \vec{d}_{K-1,m}^T\right)^T$. Therefore, $d_{k,m}$ is the transmitted data on the k-th subcarrier and m-th subsymbol, which is transmitted with a pulse shaping filter as follows

$$g_{k,m}[n] = g[(n - mK) \bmod N] \exp\left[-j\frac{2\pi kn}{K}\right], \tag{1}$$

where $g_{k,m}[n]$ represents the circularly shifted version of prototype pulse shaping filter $g[n]$. The transmitted samples are

$$x[n] = \sum_{k=0}^{K-1} \sum_{m=0}^{M-1} g_{k,m}[n]\, d_{k,m},\ 0 \le n \le N-1. \tag{2}$$

The matrix form of the equation above is

$$\vec{x} = G\vec{d}, \tag{3}$$

where G is an $N \times N$ matrix, which can be expressed as

$$G = (\vec{g}_{0,0} \cdots \vec{g}_{K-1,0} \cdots \vec{g}_{0,1} \cdots \vec{g}_{K-1,M-1}). \tag{4}$$

Finally, after adding a cyclic prefix to the GFDM signal to prevent ISI, the transmitting signal can be expressed as $\tilde{\vec{x}}$. With the assumption of linear power amplifier, perfect synchronization, and removing the cyclic prefix the received signal can be written as

$$\vec{y} = H\,\vec{x} + \vec{w}, \tag{5}$$

where $\vec{x}$ is the transmitted signal, $\vec{y}$ is the received signal, H is the $N \times N$ channel matrix, and $\vec{w}$ is additive white Gaussian noise (AWGN) with zero mean and variance σ_w^2. Assuming zero forcing equalization, the detected received signal is

$$\begin{aligned} \vec{z} &= H^{-1}HG\vec{d} + H^{-1}\vec{w} \\ &= G\vec{d} + \vec{w}, \end{aligned} \tag{6}$$

The estimated data, after GFDM demodulation, can be represented as

$$\hat{\vec{d}} = G_r\vec{z}, \tag{7}$$

where G_r is the $N \times N$ GFDM demodulation matrix. In this paper, we consider both matched filter (MF) receiver $G_r = G^H$ and zero-forcing (ZF) receiver $G_r = G^{-1}$. Finally, the estimated transmitted signal after demapping and decoding is expressed as $\hat{\vec{b}}$.

3 SIR ANALYSIS IN GFDM

In this section we derive the SIR expression for GFDM signal by considering RF impairments, namely TO, CFO, nonlinear distortion, and PN. We use m as TO, L as normalized maximum channel delay spread, N_{cp} as the length of CP, ε as normalized CFO, and ϕ_n as PN. Also to model the PN, discrete Brownian motion is considered, i.e., $[\phi[n] - \phi[n-1]] \sim \mathcal{N}(0, 2\pi\beta T_s)$, where T_s is the symbol period and β is 3-dB bandwidth.

Also, the transmitted signal with the baseband polynomial model for a memoryless nonlinear power amplifier could be expressed as[19]

$$z[n] = \sum_{i=0}^{N_p} \alpha_{2i+1} |x[n]|^{2i} x[n], \tag{8}$$

where $z[n]$ is the baseband power amplifier output signal, $x[n]$ is the power amplifier input signal, a_{2i+1} is the complex polynomial coefficient, and $2N_p + 1$ is the nonlinearity order. Since distortion due to even terms can be easily removed by filters, only odd terms are considered. Here we consider $N_p = 1$ because the third-order polynomial is enough to model the power amplifier in most practical cases[19]. Then, the power amplifier output is as follows

$$z[n] = \sum_{i=0}^{2N_p+1} \alpha_{2i+1} |x[n]|^{2i} x[n] = \alpha_1 x[n] + \alpha_3 |x[n]|^2 x[n] = \alpha_1\, x[n] + \alpha_3\, w[n], \tag{9}$$

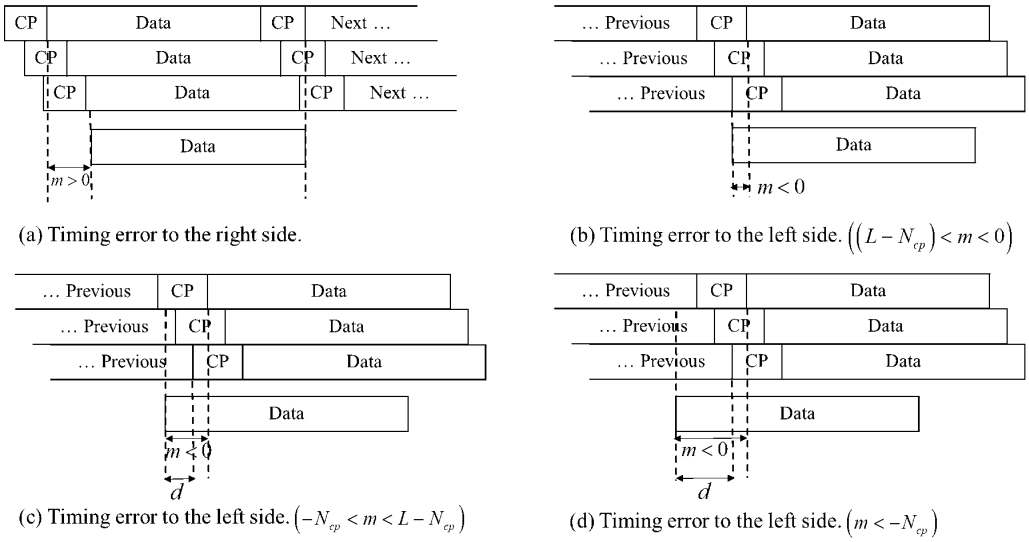

(a) Timing error to the right side.

(b) Timing error to the left side. $\left(\left(L - N_{cp}\right) < m < 0\right)$

(c) Timing error to the left side. $\left(-N_{cp} < m < L - N_{cp}\right)$

(d) Timing error to the left side. $\left(m < -N_{cp}\right)$

Fig. 2 Four cases of timing offset.[15]

where $w[n]$ is the nonlinear term.

As shown in Fig. 2, TO can be divided into four cases depending on symbol starting point estimation. Therefore, these cases are: symbol starting point estimation after the actual starting point ($m > 0$) and symbol starting point estimation before the actual starting point, which include $L - N_{cp} < m < 0$, $-N_{cp} < m < L - N_{cp}$, and $m < -N_{cp}$. Also, we assume that phase noise, TO, and CFO occur at the receiver.

3.1 Symbol starting point estimation after the actual starting point ($m > 0$):

The received GFDM signal with perfect time and frequency synchronization and a linear power amplifier, can be written as (5). We first consider the case that the symbol starting point estimation is after the actual starting point with $m > 0$ as depicted in Fig. 2-(a). Then, by extending (5) to consider the synchronization errors, phase noise, and the power amplifier distortion model of (9), the received signal in vector form can be expressed as

$$r = CP\left(R_1 H\left(\alpha_1 G d\right) + R_2\left[\begin{array}{cc} H_1 & H_2 \end{array}\right]\left[\begin{array}{c} \alpha_1 G_1 d^{next} \\ \alpha_1 G_2 d \end{array}\right] + H\left(\alpha_3 W\right)\right) + n, \tag{10}$$

where $C \in \mathbb{C}^{N\times N}$ is the CFO matrix, d^{next} is the vector of the next GFDM symbol, $P \in \mathbb{C}^{N\times N}$ is the PN matrix, $R_1, R_2 \in \mathbb{C}^{N\times N}$ are TO matrices, $G_1 \in \mathbb{C}^{(N-L)\times N}$ and $G_2 \in \mathbb{C}^{L\times N}$ are submatrices of G, and W is the vector of nonlinear distortion. These matrices can be expressed as

$$\begin{aligned}
&C = diag\left(\left[\begin{array}{cccc} 1 & e^{\frac{j2\pi\varepsilon}{K}} & \ldots & e^{\frac{j2\pi\varepsilon(N-1)}{K}} \end{array}\right]\right),\ P = diag\left(\left[\begin{array}{cccc} e^{j\phi_0} & e^{j\phi_1} & \ldots & e^{j\phi_{N-1}} \end{array}\right]\right), \\
&R_1 = \left[\begin{array}{cc} 0_{(N-m)\times m} & \mathrm{I}_{(N-m)} \\ 0_m & 0_{m\times(N-m)} \end{array}\right],\ R_2 = \left[\begin{array}{cc} 0_{(N-m)\times m} & 0_{(N-m)} \\ \mathrm{I}_m & 0_{m\times(N-m)} \end{array}\right], \\
&G_1 = \left[\begin{array}{c} G\left(\left(N - N_{cp} + 1\right) : N, :\right) \\ G\left(1 : \left(N - N_{cp} - L\right), :\right) \end{array}\right],\ G_2 = G\left(\left(N - L + 1 : N\right), :\right), \\
&W = \left[W[0]\ \cdots\ W[N-1]\right]^T.
\end{aligned} \tag{11}$$

Using (10), after zero forcing equalization and GFDM demodulation, the estimated data $\hat{d}$ becomes

$$\begin{aligned}\hat{d} &= G_r H^{-1} r \\ &= \alpha_1 G_r H^{-1} CP\left(R_1 HGd + R_2 H_1 G_1 d^{next} + R_2 H_2 G_2 d\right) + \alpha_3 G_r H^{-1} CPHW + G_r H^{-1} n \\ &= B_1 d + B_2 d^{next} + B_3 W + \hat{n},\end{aligned} \tag{12}$$

where $H_1 \in \mathbb{C}^{N\times(N-L)}$ and $H_2 \in \mathbb{C}^{N\times L}$ are the submatrices of $H = \begin{bmatrix} H_1 & H_2 \end{bmatrix}$, and B_1, B_2, B_3, and $\hat{n}$ are given respectively as

$$\begin{aligned} B_1 &= G_r H^{-1} CP\left(R_1 HG + R_2 H_2 G_2\right), \\ B_2 &= G_r H^{-1} CP R_2 H_1 G_1, \\ B_3 &= G_r H^{-1} CPH, \\ \hat{n} &= G_r H^{-1} n. \end{aligned} \tag{13}$$

We can rewrite B_1, B_2, B_3, and $\hat{d}$ as

$$\begin{aligned} &B_1 = B_L P B_{r_1},\ B_2 = B_L P B_{r_2},\ B_3 = B_L P\, B_{r_3}, \\ &\hat{d} = \alpha_1 B_L P B_{r_1} d + \alpha_1 B_L P B_{r_2} d^{next} + \alpha_3 B_L P\, B_{r_3} W + \hat{n}. \end{aligned} \tag{14}$$

where $B_L = G_r H^{-1} C, B_{r_1} = R_1 HG + R_2 H_2 G_2, B_{r_2} = R_2 H_1 G_1$, and $B_{r_3} = H$.

Theorem 1*: The SIR for GFDM by considering RF impairments, namely TO, CFO, nonlinear distortion, and PN for the case of $m > 0$ can be obtained as follows*

$$\Gamma\left(m, \varepsilon, \beta T_s\right) = \frac{|\alpha_1|^2 \sum_{i=0}^{N-1} \sum_{j=0}^{N-1} e^{-\frac{\pi\beta T_s |i-j|}{N}} \times a_{r_1,j}^H a_{r_1,i}}{I_1}, \tag{15}$$

with

$$\begin{aligned} I_1 = |\alpha_1|^2 \sum_{i=0}^{N-1} \sum_{j=0}^{N-1} e^{-\frac{\pi\beta T_s |i-j|}{N}} \left(1_N^T \left(A_{r_1,i} \circ A_{r_1,j}^* + A_{r_2,i} \circ A_{r_2,j}^*\right) 1_N - a_{r_1,j}^H a_{r_1,i}\right) \\ + |\alpha_3|^2 \sum_{i=0}^{N-1} \sum_{j=0}^{N-1} e^{-\frac{\pi\beta T_s |i-j|}{N}} \left(1_N^T \left(A_{r_3,i} \circ A_{r_3,j}^*\right) 1_N\right) \sum_{k=0}^{N-1} \left(\sigma_W^2\right)_k. \end{aligned}$$

where $A_{r_j,i} = b_{L,i}\, b_{r_j,i}^T$, $a_{r_1,i} = diag\left(b_{L,i}\, b_{r_1,i}^T\right)$, $b_{L,i-1}$ is the i^{th} column vector of B_L, $b_{r_j,i-1}^T$ is the i^{th} row vector of B_{r_j}.

Proof: The proof is provided in Appendix.

3.2 Symbol starting point estimation before the actual starting point ($(L - N_{cp}) < m < 0$):

We first consider the case that the symbol starting point estimation is before the actual starting point with $(L - N_{cp}) < m < 0$. As depicted in Fig. 2-(b), TO does not occur in this case, however, ISI and ICI are created due to non-orthogonal waveform of GFDM. Then, by extending (5) to consider the synchronization errors, phase noise, and the power amplifier distortion model of (9), the received signal in vector form is obtained as follows

$$r = CP\left[\left(R_1^l H + R_2^l H M_{N_{cp}}\right) \alpha_1 Gd + \alpha_3 HW\right] + n, \tag{16}$$

where R_1^l and $R_2^l \in \mathbb{C}^{N\times N}$ are TO matrices and $M_{N_{cp}}$ is the matrix that shifts the elements of Gd circularly, which are given as

$$R_1^l = \begin{bmatrix} 0_{|m|\times(N-|m|)} & 0_{|m|} \\ \mathrm{I}_{N-|m|} & 0_{(N-|m|)\times|m|} \end{bmatrix},$$

$$R_2^l = \begin{bmatrix} 0_{|m|\times(N_{cp}-|m|)} \ \mathrm{I}_{|m|} \ 0_{|m|\times(N-N_{cp})} \\ 0_{(N-|m|)\times N} \end{bmatrix}, \tag{17}$$

$$M_{N_{cp}} = \begin{bmatrix} 0_{N_{cp}\times(N-N_{cp})} & \mathrm{I}_{N_{cp}} \\ \mathrm{I}_{N-N_{cp}} & 0_{\left(N-N_{cp[}\right)\times N_{cp}} \end{bmatrix}.$$

Using (16), after zero forcing equalization and GFDM demodulation, the estimated data $\hat{d}$ is

$$\begin{aligned} \hat{d} &= G_r H^{-1} CP \left[\left(R_1^l H + R_2^l H M_{N_{cp}} \right) \alpha_1 G d + \alpha_3 H W \right] + \hat{n} \\ &= \alpha_1 B_L P B_{l_1} d + \alpha_3 B_L P B_{l_2} W + \hat{n}, \end{aligned} \tag{18}$$

where $B_{l_1} = \left(R_1^l H + R_2^l H M_{Ncp} \right) G$ and $B_{l_2} = H$.

Theorem 2*: The SIR for GFDM by considering RF impairments, namely TO, CFO, nonlinear distortion, and PN for the case of* $(L - N_{cp}) < m < 0$ *can be obtained as follows*

$$\Gamma\left(m, \varepsilon, \beta T_s\right) = \frac{|\alpha_1|^2 \sum_{i=0}^{N-1} \sum_{j=0}^{N-1} e^{-\frac{\pi\beta T_s|i-j|}{N}} \times a_{l_1,j}^H a_{l_1,i}}{I_2}, \tag{19}$$

with

$$\begin{aligned} I_2 = |\alpha_1|^2 \sum_{i=0}^{N-1} \sum_{j=0}^{N-1} e^{-\frac{\pi\beta T_s|i-j|}{N}} \left(1_N^T \left(A_{l_1,i} \circ A_{l_1,j}^* \right) 1_N - a_{l_1,j}^H a_{l_1,i} \right) \\ + |\alpha_3|^2 \sum_{i=0}^{N-1} \sum_{j=0}^{N-1} e^{-\frac{\pi\beta T_s|i-j|}{N}} \left(1_N^T \left(A_{l_2,i} \circ A_{l_2,j}^* \right) 1_N \right) \sum_{k=0}^{N-1} \left(\sigma_W^2 \right)_k. \end{aligned}$$

where $A_{l_j,i} = b_{L,i}\, b_{l_j,i}^T$, $a_{l_1,i} = diag\left(b_{L,i}\, b_{l_1,i}^T \right)$, $b_{L,i-1}$ is the i^{th} column vector of B_L, $b_{l_j,i-1}^T$ is the i^{th} row vector of B_{l_j}.

Proof: The proof is similar to that of Theorem 1.

3.3 Symbol starting point estimation before the actual starting point $(-N_{cp} < m < (L - N_{cp}))$:

We first consider the case that the symbol starting point estimation is before the actual starting point with $-N_{cp} < m < (L - N_{cp})$. As depicted in Fig. 2-(c), ISI and ICI exist in this case due to the missing samples of the current GFDM symbol. Then, by extending (5) to consider the synchronization errors, phase noise, and the power amplifier distortion model of (9), the received signal in vector form in this case is obtained as follows

$$r = CP \left(\left(R_1^l H + R_3^l H M_{N_{cp}} \right) \alpha_1 G d + R_4^l H \begin{bmatrix} \alpha_1 G_1 d \\ \alpha_1 G_2 d^{prev} \end{bmatrix} + \alpha_3 H W \right) + n, \tag{20}$$

where R_3^l and $R_4^l \in \mathbb{C}^{N\times N}$ are TO matrices given as

$$R_3^l = \begin{bmatrix} 0_{(L-N_{cp}+|m|)\times N} \\ 0_{(N_{cp}-L)\times L} \ \mathrm{I}_{(N_{cp}-L)} \ 0_{(N_{cp}-L)\times(N-N_{cp})} \\ 0_{(N-|m|)\times N} \end{bmatrix},$$

$$R_4^l = \begin{bmatrix} 0_{\omega\times(N_{cp}-|m|)} \ \mathrm{I}_{\omega} \ 0_{\omega\times(N-N_{cp})} \\ 0_{(N-\omega)\times N} \end{bmatrix}. \tag{21}$$

Using (20), the estimated data $\hat{d}$ after zero forcing equalization is

$$\begin{aligned}\hat{d} &= G_r H^{-1} CP \left(\left(R_1^l H + R_3^l H M_{N_{cp}} \right) \alpha_1 G d + R_4^l H \begin{bmatrix} \alpha_1 G_1 d \\ \alpha_1 G_2 d^{prev} \end{bmatrix} + \alpha_3 H W \right) + \hat{n} \\ &= \alpha_1 B_L P B_{l_3} d + \alpha_1 B_L P B_{l_4} d^{prev} + \alpha_3 B_L P B_{l_5} W + \hat{n},\end{aligned} \tag{22}$$

where $B_{l_3} = \left(R_1^l H G + R_3^l H M_{Ncp} G + R_4^l H_1 G_1 \right)$, $B_{l_4} = R_4^l H_2 G_2$, and $B_{l_5} = H$. Since the equation above is similar to (14), its SIR expression is obtained in a similar manner to (15) as:

$$\Gamma\left(m, \varepsilon, \beta T_s\right) = \frac{|\alpha_1|^2 \sum_{i=0}^{N-1} \sum_{j=0}^{N-1} e^{-\frac{\pi \beta T_s |i-j|}{N}} \times a_{l_3,j}^H a_{l_3,i}}{I_3}, \tag{23}$$

with

$$\begin{aligned}I_3 = |\alpha_1|^2 \sum_{i=0}^{N-1} \sum_{j=0}^{N-1} e^{-\frac{\pi \beta T_s |i-j|}{N}} \left(1_N^T \left(A_{l_3,i} \circ A_{l_3,j}^* + A_{l_4,i} \circ A_{l_4,j}^* \right) 1_N - a_{l_3,j}^H a_{l_3,i} \right) \\ + |\alpha_3|^2 \sum_{i=0}^{N-1} \sum_{j=0}^{N-1} e^{-\frac{\pi \beta T_s |i-j|}{N}} \left(1_N^T \left(A_{l_5,i} \circ A_{l_5,j}^* \right) 1_N \right) \sum_{k=0}^{N-1} \left(\sigma_W^2 \right)_k.\end{aligned}$$

where $A_{l_j,i} = b_{L,i}\, b_{l_j,i}^T$, $a_{l_3,i} = diag\left(b_{L,i}\, b_{l_3,i}^T \right)$, $b_{L,i-1}$ is the i^{th} column vector of B_L, $b_{l_j,i-1}^T$ is the i^{th} row vector of B_{l_j}.

3.4 Symbol starting point estimation before the actual starting point ($m < -N_{cp}$):

We first consider the case that the symbol starting point estimation is before the actual starting point with $m < -N_{cp}$. As depicted in Fig. 2-(d), ISI exist in this case due to TO choosing some samples of the previous GFDM symbol. Then, by extending (5) to consider the synchronization errors, phase noise, and the power amplifier distortion model of (9), the received signal in vector form is obtained as follows

$$r = CP \left(\left(R_1^l H + R_3^l H M_{N_{cp}} \right) \alpha_1 G d + R_5^l H \begin{bmatrix} \alpha_1 G_1 d \\ \alpha_1 G_2 d^{prev} \end{bmatrix} + R_6^l H \alpha_1 G d^{prev} + \alpha_3 H W \right) + n, \tag{24}$$

where R_5^l and $R_6^l \in \mathbb{C}^{N \times N}$ are TO matrices given as

$$\begin{aligned}R_5^l &= \begin{bmatrix} 0_{(|m|-N_{cp}) \times N} \\ \mathrm{I}_L \; 0_{L \times (N-L)} \\ 0_{(N-\omega) \times N} \end{bmatrix}, \\ R_6^l &= \begin{bmatrix} 0_{(|m|-N_{cp}) \times (N-|m|+N_{cp})} \; \mathrm{I}_{(|m|-N_{cp})} \\ 0_{(N-|m|+N_{cp}) \times N} \end{bmatrix}.\end{aligned} \tag{25}$$

Using (23), the estimated data $\hat{d}$after zero forcing equalization is

$$\begin{aligned}\hat{d} &= G_r H^{-1} CP \left(\left(R_1^l H + R_3^l H M_{N_{cp}} \right) \alpha_1 G d + R_5^l H \begin{bmatrix} \alpha_1 G_1 d \\ \alpha_1 G_2 d^{prev} \end{bmatrix} + R_6^l H \alpha_1 G d^{prev} + \alpha_3 H W \right) + \hat{n} \\ &= \alpha_1 B_L P B_{l_6} d + \alpha_1 B_L P B_{l_7} d^{prev} + \alpha_3 B_L P B_{l_8} W + \hat{n},\end{aligned} \tag{26}$$

where $B_{l_6} = \left(R_1^l H G + R_3^l H M_{N_{cp}} G + R_5^l H_1 G_1 \right)$, $B_{l_7} = R_5^l H_2 G_2 + R_6^l H G$, and $B_{l_8} = H$. SIR in this case is similar to (15).

$$\Gamma\left(m,\varepsilon,\beta T_s\right)=\frac{|\alpha_1|^2\sum_{i=0}^{N-1}\sum_{j=0}^{N-1}e^{-\frac{\pi\beta T_s|i-j|}{N}}\times a_{l_6,j}^H a_{l_6,i}}{I_4}, \tag{27}$$

with

$$I_4=|\alpha_1|^2\sum_{i=0}^{N-1}\sum_{j=0}^{N-1}e^{-\frac{\pi\beta T_s|i-j|}{N}}\left(1_N^T\left(A_{l_6,i}\circ A_{l_6,j}^*+A_{l_7,i}\circ A_{l_7,j}^*\right)1_N-a_{l_6,j}^H a_{l_6,i}\right)$$

$$+|\alpha_3|^2\sum_{i=0}^{N-1}\sum_{j=0}^{N-1}e^{-\frac{\pi\beta T_s|i-j|}{N}}\left(1_N^T\left(A_{l_8,i}\circ A_{l_8,j}^*\right)1_N\right)\sum_{k=0}^{N-1}\left(\sigma_W^2\right)_k.$$

where $A_{l_j,i}=b_{L,i}\,b_{l_j,i}^T$, $a_{l_6,i}=diag\left(b_{L,i}\,b_{l_6,i}^T\right)$, $b_{L,i-1}$ is the i^{th} column vector of B_L, $b_{l_j,i-1}^T$ is the i^{th} row vector of B_{l_j}.

4 SIMULATION RESULTS

We compare the effects of synchronization errors, PN, and nonlinear distortion on SIR of GFDM and OFDM systems. In our simulations, we consider $K=32$, $M=5$, $N_{cp}=24$, and for GFDM, a pulse shaping filter of root raised cosine with roll-off factor of 0.1. We use also 32-point fast fourier transform (FFT) and $N_{cp}=24$ for OFDM to ensure a fair comparison with GFDM. The Rayleigh fading channel is assumed with 10 channel taps and exponential power delay profile with $\beta e^{-l/L}$ for $0\leq l\leq L$ where β is $\sum_{l=0}^{L}(\beta e^{-l/L})^2=1$. Also, to place the transmitter in the nonlinear region, we considered the maximum input power of the PA to be 2.5 dB less than the saturation point of the nonlinear PA model.

We use $\varepsilon=0.1$, $\beta T_s=0.01$, $m=1$, $\alpha_1=1.0108+0.0858\text{j}$, $\alpha_3=0.0879-0.1583\text{j}$, also we consider both matched filter (MF) receiver $G_r=G^H$ and zero-forcing (ZF) receiver $G_r=G^{-1}$ for our simulations. As mentioned in [15] and can be seen in our simulation results, GFDM is most sensitive to CFO, while it is robust to TO and PN.

Fig. 3 shows SIR versus TO. As can be seen, OFDM performs better than GFDM for low TOs, since TO in addition to ICI and ISI creates inter-subsymbol interference in GFDM. However, for high TOs, the OFDM performance decreases since its symbol length is less than that of GFDM, which in turn increases the interference with the next symbol.

In Fig. 4, the effects of CFO on SIR is analyzed. In Equation (11), CFO matrix in GFDM shows, as the symbol length increases, the phase shift of data caused by CFO increases which leads to inferior performance of GFDM compared to OFDM.

The SIR versus PN variance is presented in Fig. 5. The GFDM performance is better with PN compared to OFDM since the symbol period, T_s of OFDM is longer than that of GFDM. It can be observed from the PN model introduced in Section III that the phase noise impact on the OFDM signal is enhanced by the relatively long symbol period of T_s compared with GFDM signal.

Fig. 6 represents the SIR versus nonlinear distortion. High PAPR degrades the performance of communication systems. As mentioned in [3], a lower PAPR is achieved employing GFDM compared to OFDM, assuming linear power amplifiers. However, as shown in [20,21], GFDM systems have high PAPR with nonlinear amplifiers, which leads to an inferior performance compared to the OFDM system, which is also observed in Fig. 6.This increase in PAPR (hence decrease in performance) can be due to larger symbol length of GFDM compared to OFDM.

Note that here we have just analyzed the GFDM performance for two common receiver filters, namely MF and ZF. However, by designing a SIR maximizing filter (obtaining the filter by solving an optimization with the objective of SIR), GFDM can outperform OFDM, though with higher computational complexity.

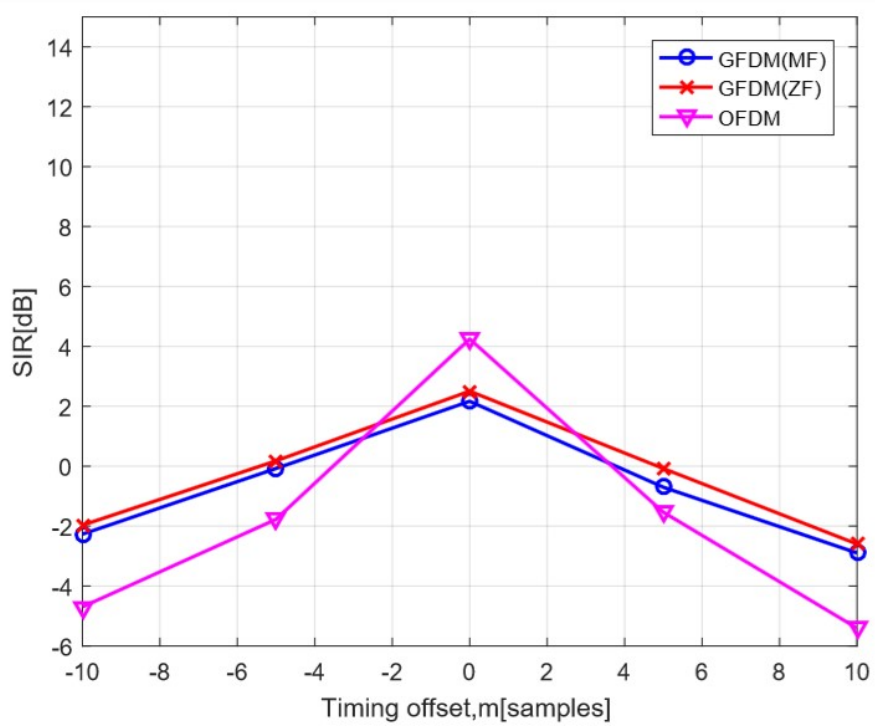

Fig. 3 SIR versus TO

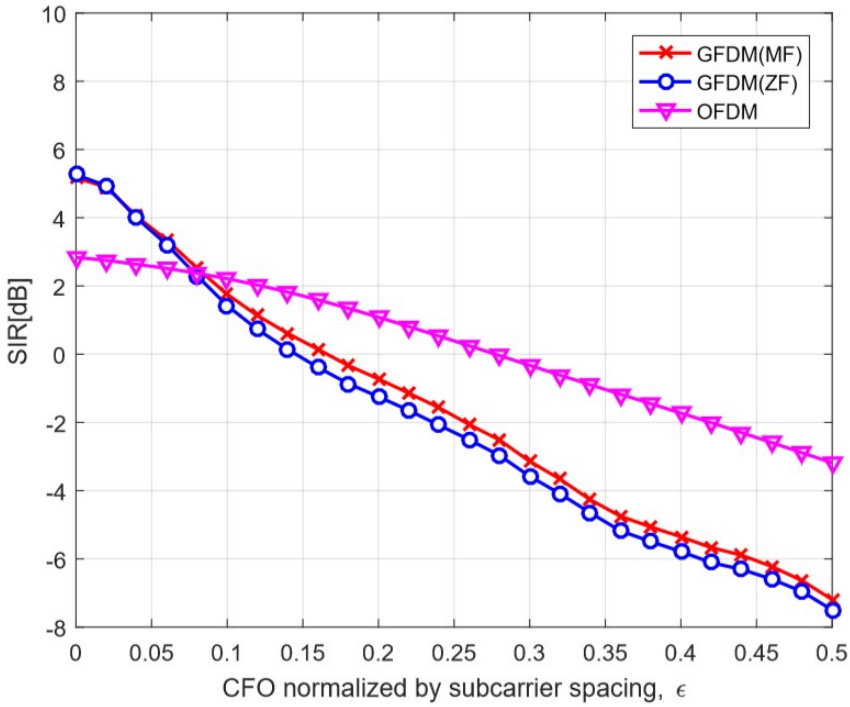

Fig. 4 SIR versus CFO

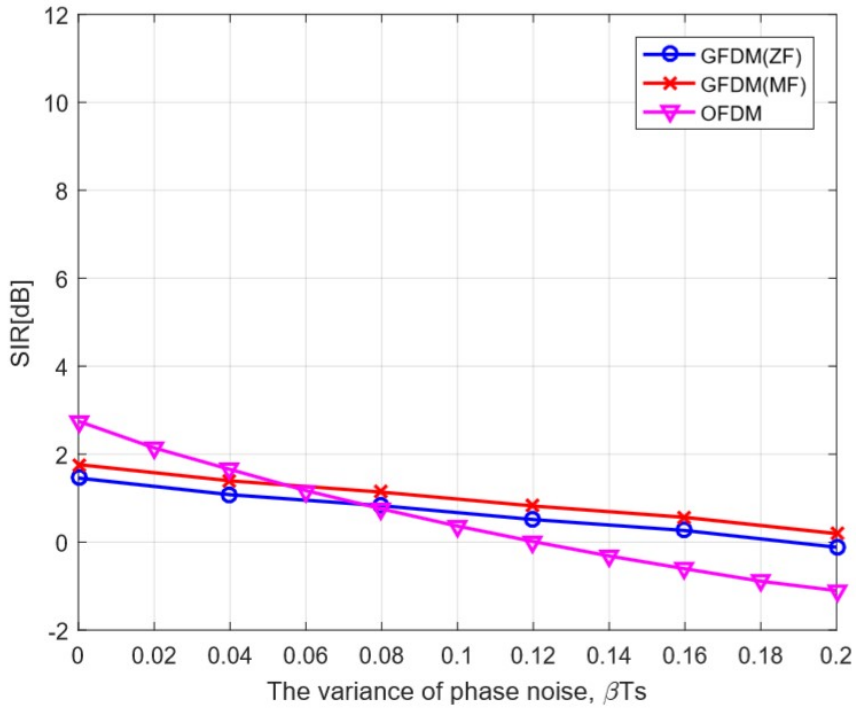

Fig. 5 SIR versus PN

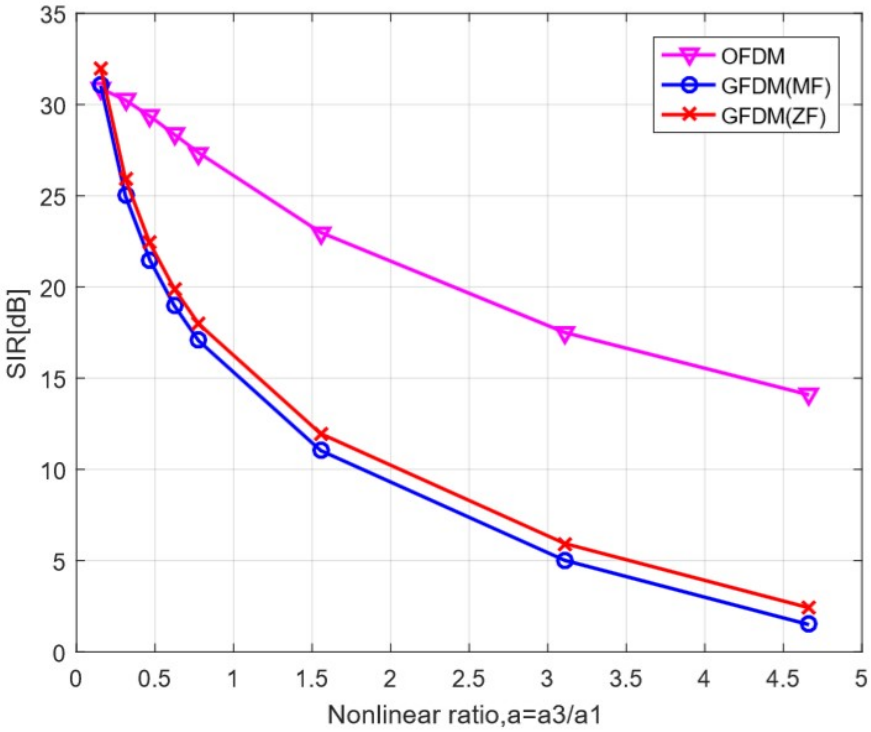

Fig. 6 SIR versus nonlinear distortion

5 CONCLUSION

In this paper, we have derived close-form expressions of the SIR for GFDM waveforms by considering RF impairments, namely TO, CFO, PN, and nonlinear distortion and analyzed the effects of synchronization errors, PN, and nonlinear distortion for GFDM and OFDM systems. Based on the simulations, GFDM based systems are more sensitive to CFO and nonlinear distortion than OFDM based systems, while the GFDM based systems are more robust to TO and PN. Therefore, the results presented in this paper can be a good guideline for waveform design in the next generation of communication systems. An extension of this work can include the comparison of combined effects of TO, CFO, PN and non-linearity with the common additive aggregate linear models for hardware impairments.

APPENDIX

The estimated data for l^{th} symbol in (12) is

$$\hat{d}_l = \underbrace{\alpha_1 [B_1]_{l,l} d_l}_{S_l} + \underbrace{\alpha_1 \sum_{\substack{k=0 \\ k\neq l}}^{N-1} [B_1]_{l,k} d_k}_{I_l} + \underbrace{\alpha_1 \sum_{k=0}^{N-1} [B_2]_{l,k} d_k^{next}}_{P_l} + \underbrace{\alpha_3 \sum_{k=0}^{N-1} [B_3]_{l,k} (W)_k}_{N_l} + \hat{n}_l, \tag{28}$$

where d_K is the zero-mean i.i.d. data symbol with unit variance on the K-th symbol and S_l is the desired signal term, I_l, and P_l are unwanted signals, which represent the ISI and ICI introduced by synchronization errors and PN, and N_l is the nonlinear distortion noise due to the nonlinearity of the power amplifier.

$$\begin{aligned} \Gamma_l\left(m, \varepsilon, \beta T_s\right) &= \frac{\mathrm{E}\left[|S_l|^2\right]}{\mathrm{E}\left[|I_l|^2\right] + \mathrm{E}\left[|P_l|^2\right] + \mathrm{E}\left[|N_l|^2\right]} \\ &= \frac{|\alpha_1|^2 \mathrm{E}\left[\left|[B_1]_{l,l}\right|^2\right]}{|\alpha_1|^2 \mathrm{E}\left[\sum\limits_{\substack{k=0 \\ k\neq l}}^{N-1} \left|[B_1]_{l,k}\right|^2\right] + |\alpha_1|^2 \mathrm{E}\left[\sum\limits_{k=0}^{N-1} \left|[B_2]_{l,k}\right|^2\right] + |\alpha_3|^2 \mathrm{E}\left[\sum\limits_{k=0}^{N-1} \left|[B_3]_{l,k}\right|^2\right] \sum\limits_{k=0}^{N-1} \left(\sigma_W^2\right)_k}, \end{aligned} \tag{29}$$

where $B_1 = B_L P B_{r_1}$, $B_2 = B_L P B_{r_2}$, $B_3 = B_L P\, B_{r_3}$, $B_L = G_r H^{-1} C$, $B_{r_1} = R_1 H G + R_2 H_2 G_2$, $B_{r_2} = R_2 H_1 G_1$, and $B_{r_3} = (R_1 + R_2)\, H$. Then, B_1 can be written as

$$\begin{aligned} B_1 &= B_L P B_{r_1} \\ &= \left[\, b_{L,0}\; b_{L,1}\; \ldots\; b_{L,N-1} \,\right] P \begin{bmatrix} b_{r_1,0}^T \\ b_{r_1,1}^T \\ \vdots \\ b_{r_1,N-1}^T \end{bmatrix} \\ &= \sum_{i=0}^{N-1} e^{j\phi_i} b_{L,i} b_{r_1,i}^T, \end{aligned} \tag{30}$$

where $b_{L,i-1}$ is the i^{th} column vector of B_L and $b_{r_1,i-1}^T$ is the i^{th} row vector of B_{r_1}. Using (28), the power of S_l in (27) can be written as

$$\begin{aligned}\mathrm{E}\left[|S_l|^2\right] &= |\alpha_1|^2 \mathrm{E}\left[\left|[B_1]_{l,l}\right|^2\right] \\ &= |\alpha_1|^2 \sum_{i=0}^{N-1}\sum_{j=0}^{N-1} \mathrm{E}\left[e^{j(\phi_i-\phi_j)}\right] \mathrm{E}\left[\left[b_{L,i}b_{r_1,i}^T\right]_{l,l}\left[b_{L,j}b_{r_1,j}^T\right]_{l,l}^*\right] \\ &= \tfrac{|\alpha_1|^2}{N} \sum_{i=0}^{N-1}\sum_{j=0}^{N-1} e^{-\frac{\pi\beta T_s|i-j|}{N}} \times a_{r_1,j}^H a_{r_1,i},\end{aligned} \tag{31}$$

where $a_{r_1,i} = diag\left(b_{L,i}b_{r_1,i}^T\right)$. The power of I_l by using (28) can be written as

$$\begin{aligned}\mathrm{E}\left[|I_l|^2\right] &= |\alpha_1|^2 \mathrm{E}\left[\sum_{\substack{k=0\\k\neq l}}^{N-1}\left|[B_1]_{l,k}\right|^2\right] \\ &= |\alpha_1|^2 \sum_{i=0}^{N-1}\sum_{j=0}^{N-1} e^{-\frac{\pi\beta T_s|i-j|}{N}} \left(\sum_{k=0}^{N-1}\mathrm{E}\left[[A_{r_1,i}]_{l,k}\left[A_{r_1,j}\right]_{l,k}^*\right] - \mathrm{E}\left[[A_{r_1,i}]_{l,l}\left[A_{r_1,j}\right]_{l,l}^*\right]\right) \\ &= \tfrac{|\alpha_1|^2}{N} \sum_{i=0}^{N-1}\sum_{j=0}^{N-1} e^{-\frac{\pi\beta T_s|i-j|}{N}} \left(1_N^T\left(A_{r_1,i}\circ A_{r_1,j}^*\right)1_N - a_{r_1,j}^H a_{r_1,i}\right),\end{aligned} \tag{32}$$

where $A_{r_1,i} = b_{L,i}b_{r_1,i}^T$. The power of P_l by using (28) can be calculated as

$$\begin{aligned}\mathrm{E}\left[|P_l|^2\right] &= |\alpha_1|^2 \mathrm{E}\left[\sum_{k=0}^{N-1}\left|[B_2]_{l,k}\right|^2\right] \\ &= \tfrac{|\alpha_1|^2}{N} \sum_{i=0}^{N-1}\sum_{j=0}^{N-1} e^{-\frac{\pi\beta T_s|i-j|}{N}} \left(1_N^T\left(A_{r_2,i}\circ A_{r_2,j}^*\right)1_N\right),\end{aligned} \tag{33}$$

where $A_{r_2,i} = b_{L,i}b_{r_2,i}^T$. The power of N_l can be calculated as

$$\begin{aligned}\mathrm{E}\left[|N_l|^2\right] &= |\alpha_3|^2 \mathrm{E}\left[\sum_{k=0}^{N-1}\left|[B_3]_{l,k}(W)_k\right|^2\right] \\ &= |\alpha_3|^2 \mathrm{E}\left[\sum_{k=0}^{N-1}\left|[B_3]_{l,k}\right|^2\right]\sum_{k=0}^{N-1}\left(\sigma_W^2\right)_k \\ &= \tfrac{|\alpha_3|^2}{N} \sum_{i=0}^{N-1}\sum_{j=0}^{N-1} e^{-\frac{\pi\beta T_s|i-j|}{N}} \left(1_N^T\left(A_{r_3,i}\circ A_{r_3,j}^*\right)1_N\right)\sum_{k=0}^{N-1}\left(\sigma_W^2\right)_k,\end{aligned} \tag{34}$$

where $A_{r_3,i} = b_{L,i}b_{r_3,i}^T$. Also, the power of the nonlinear distortion is

$$\sum_{k=0}^{N-1}\left(\sigma_W^2\right)_k = \sum_{k=0}^{N-1} E\left[W_k\, W_k^*\right] = \sum_{k=0}^{N-1} E\left[|x_k|^2 x_k \quad |x_k|^2 x_k\right]. \tag{35}$$

Lemma: Suppose z_n for $n = 1, 2, \cdots, N$ are zero-mean complex Gaussian RVs.
a) If $n \neq m$, then

$$E\left[z_1\, z_2\, , ...,\, z_n\, z_1^*\, z_2^*,\, \ldots,\, z_m^*\right] = 0, \quad n, m = 1, 2, \cdots, N \tag{36}$$

b) If $n = m$, then

$$E\left[z_1\, z_2\, , ...\, , z_n\, z_1^*\, z_2^*,\, \ldots\, , z_m^*\right] = \sum_{\pi} E\left[z_{\pi(1)}z_1^*\right] E\left[z_{\pi(2)}z_2^*\right], \ldots, E\left[z_{\pi(n)}z_m^*\right], \tag{37}$$

where π is a permutation of $\{1, 2, 3, \cdots, m\}$ (a set of integers).

Proof: By utilizing moments of complex Gaussian random variable (RV) z, the Lemma is given in[22].
By considering (2), $x[n]$ is a summation of MK i.i.d. RVs. Due to central limit theorem[23] as MK gets large, the distributions of $x[n]$ tends to Gaussian. Due to Gaussian distribution of $x[n]$, above Lemma can be used to further simplify (33) as follows

$$\begin{aligned} &E\left[(x[n])^{i_1+1}x[n]^{i_2}(x^*[n])^{i_2+1}x^*[n]^{i_1}\right] = \\ &\sum_{\pi} E\left[x_{\pi(1)}x^*[n]\right],\ldots,E\left[x_{\pi(i_1)}x^*[n]\right]E\left[x_{\pi(i_1+1)}x^*[n]\right],\ldots,E\left[x_{\pi(i_1+i_2+1)}x^*[n]\right] \end{aligned} \tag{38}$$

where $n = m = i_1 + i_2 + 1$ and $x_i = x[n]$ for $i = 1,\ldots,i_1+i_2+1$. Using (36) and After some calculations, we obtain

$$\begin{aligned} &E\left[(x[n])^{i_1+1}x[n]^{i_2}(x^*[n])^{i_2+1}x^*[n]^{i_1}\right] = \\ &\sum_{p=0}^{\min(i_1,i_2)} \binom{i_2+1}{p+1}\binom{i_1+1}{p+1}\binom{i_2}{p}\binom{i_1}{p} \\ &(p+1)!\,(p)!\,(i_2-p)!\,(i_1-p)!(R_{xx}(0))^{p+1}(R_{xx}^*(0))^p(R_{xx}(0))^{i_1+i_2-2p}, \end{aligned} \tag{39}$$

By considering the third order nonlinearity, (33) can be written as

$$E\left[(x[n])^2 x[n]\ (x^*[n])^2 x^*[n]\right] = 4\left[(R_{xx}[0])^3\right] + 2\left[(R_{xx}[0])^2 R_{xx}^*[0]\right]. \tag{40}$$

By using (2), the autocorrelation function is written as follows

$$\begin{aligned} &R_{xx}[0] = E[x[n]\,x^*[n]] \\ &= \sum_{k_1=0}^{K-1}\sum_{k_2=0}^{K-1}\sum_{m_1=0}^{M-1}\sum_{m_2=0}^{M-1} E\left[d_{k,m}d_{k,m}^*\right] g_{m_1}[n]\,g_{m_2}^*[n] \quad \times e^{j2\pi\frac{k_1}{K}n}e^{-j2\pi\frac{k_2}{K}n}. \end{aligned} \tag{41}$$

Since data symbol $d_{k,m}$ is an i.i.d. RV, we have

$$E\left[d_{k,m}d_{k,m}^*\right] = \delta(k_1-k_2)\,\delta(m_1-m_2), \tag{42}$$

By considering (39), (38) has nonzero value for $k_1 = k_2 = k, m_1 = m_2 = m$. Thus, we have

$$R_{xx}[0] = \sum_{k=0}^{K-1}\sum_{m=0}^{M-1} g_m[n]\,g_m^*[n] = K\sum_{m=0}^{M-1} g_m[n]\,g_m^*[n] = K\sum_{m=0}^{M-1}|g_m[n]|^2. \tag{43}$$

Substituting (29), (30), (31), and (32) into (27), we can obtain SIR as given by (15).

References

1. G. Wunder, Jung, et al, 5gnow: Non-orthogonal, asynchronous waveforms for future mobile applications, IEEE Communications Magazine, 52, 97-105 (2014).
2. J. G. Andrews, et al, What will 5g be?, IEEE Journal on Selected Areas in Communications, 32, 1065-1082 (2014).
3. Gfdm performance in terms of ber, papr and oob and comparison to ofdm system, 1715 (2016).
4. S. A. Fechtel, A. Blaickner, Efficient fft and equalizer implementation for ofdm receivers, IEEE Transactions on Consumer Electronics 45, 1104-1107 (1999).
5. Z. You, J. Fang, I. T. Lu, Out-of-band emission suppression techniques based on a generalized ofdm framework, Eurasip Journal on Advances in Signal Processing, 2014, 1-14 (2014).
6. N. Michailow, M. Matthe, I. S. Gaspar, A. N. Caldevilla, L. L. Mendes, A. Festag, G. Fettweis, Generalized frequency division multiplexing for 5th generation cellular networks, IEEE Transactions on Communications, 62, 3045-3061 (2014).
7. B. Farhang-Boroujeny, Ofdm versus filter bank multicarrier, IEEE Signal Processing Magazine, 28, 92-112 (2011).

8. R. Datta, and N. Michailow, and M. Lentmaier, and G. Fettweis, GFDM interference cancellation for flexible cognitive radio phy design, IEEE Vehicular Technology Conference (2012).
9. Series and Cripps Peter Aaen, The Cambridge RF and Microwave Engineering Series Characterization of RF and Microwave Power FETs Enrico Rubiola, Phase Noise and Frequency Stability in Oscillators.
10. Mostofi, Yasamin and Cox, Donald C., Mathematical analysis of the impact of timing synchronization errors on the performance of an OFDM system, journal IEEE Transactions on Communications, 54, 226-230 (2006).
11. V. Nguyen-Duy-Nhat, H. Nguyen-Le, C. Tang-Tan, T. Le-Ngoc, Sir analysis for ofdm transmission in the presence of cfo, phase noise and doubly selective fading, IEEE Communication, 17, 1810-1813 (2013).
12. K. Raghunath, A. Chockalingam, Sir analysis and interference cancellation in uplink ofdma with large carrier frequency/timing offsets, IEEE Transactions on Wireless Communications, 8, 2202-2208 (2009).
13. M. Baghani, A. Mohammadi, M. Majidi, M. Valkama, Uplink resource allocation in multiuser multicarrier cognitive radio networks under power amplifier nonlinearity, Transactions on Emerging Telecommunications Technologies, 28, 3162 (2017).
14. J. H. Choi, B. J. Lim, Y. J. Kim, Y. C. Ko, Effect of timing and frequency synchronization errors on gfdm systems, 1322-1325 (2015).
15. B. Lim, Y. C. Ko, Sir analysis of ofdm and gfdm waveforms with timing offset, cfo, and phase noise, IEEE Transactions on Wireless Communications, 16, 6979-6990 (2017).
16. H. Cheng, Y. Xia, Y. Huang, L. Yang, Z. Xiong, D. P. Mandic, Improperness based sinr analysis of gfdm systems under joint tx and rx i/q imbalance 2020-May.
17. A. Mohammadian, C. Tellambura, Full-duplex gfdm radio transceivers in the presence of phase noise, cfo and iq imbalance 2019-May.
18. S. Han, Y. Sung, Y. H. Lee, Filter design for generalized frequency-division multiplexing, IEEE Transactions on Signal Processing, 65,1644-1659 (2017).
19. A. Mohammadian, M. Baghani, C. Tellambura, Optimal power allocation of gfdm secondary links with power amplifier nonlinearity and aci, IEEE Wireless Communications, 8, 93-96 (2019).
20. Z. A. Sim, R. Reine, Z. Zang, F. H. Juwono, L. Gopal, Reducing the papr of gfdm systems with quadratic programming filter design, 2019-April.
21. L. Sendrei, S. Marchevsky, Nonlinear noise estimation and compensation in gfdm based communication systems for cognitive radio networks, 313-316(2015).
22. I. S. Reed, On a moment theorem for complex gaussian processes, IRE Transactions on Information Theory, 8,194-195 (1962).
23. K. G. Gard, Characterization of spectral regrowth in microwave amplifiers based on the nonlinear transformation of a complex gaussian process, IEEE Transactions on Microwave Theory and Techniques, 47, 1059-1069 (1999).